

Visibility of Thin Lines on Coloured Backgrounds

*R. Victor Klassen, Karen M. Braun,
Robert R. Buckley, Kalpana Janamanchi
Xerox Corporation
Webster, New York, USA*

Abstract

We measured the threshold of visibility of a thin line against a solid background. The line colour differed from that of the background in only one of L^* , C^* , and h_{ab} . The twenty-seven background colours were distributed throughout colour space. We observed trends in the dependence of the threshold differences in C^* and h_{ab} as functions of C^* and h_{ab} of the background colour. We found our best quantitative agreement resulted from a C^* and h_{ab} dependent colour difference formula, similar in spirit to the CIE94 colour difference metric, but with different parameters and weighting functions. Finally we simulated our geometry in input to an s-CIELAB implementation and found that s-CIELAB predicted our results quite well.

Introduction

We are interested in measuring the threshold visibility of small linear defects in print media, such as scratches and certain misregistration errors. Such features are most visible when they occur in a large field of a constant, contrasting colour, and take the form of long linear defects. We wish to know the threshold of visibility of a thin line, as a function of the colour of the background (base colour) against which the line appears, and the direction in colour space from the base colour to the line colour. Ideally, we would like to express the function as a (reasonably) simple expression involving the measured values L^* , a^* , and b^* of the base colour and line colour. This threshold is also likely to be a function of the line geometry (width, length, orientation), but in this study, we kept these parameters constant.

The majority of spatial acuity and contrast sensitivity work has been limited to achromatic acuity. It is well known that spatial acuity is greater for achromatic stimuli. Robson¹ gives a spatial contrast-sensitivity function, i.e. a function mapping spatial frequency to threshold contrast, but only for lightness data. Kelly² extends this work into the chromatic domain, finding the function for red-green equiluminant gratings. He found that chromatic gratings disappear when they are stabilized on the retina. We are interested in the

more common viewing condition where the eye freely saccades. Noorlander *et al*³ explored sensitivity to gratings in the red/green plane, with a single background colour (yellow), while Mullen⁴ explored red/green and blue/yellow gratings. These experiments used small numbers (2 or 3) of observers, allowing them to thoroughly characterize the sensitivity of those observers. By contrast, we used sixteen observers, which limited our ability to explore in detail the sensitivity of any one observer, but allowed us to measure averages with greater confidence.

The Commission Internationale de L'Éclairage (CIE) recommends a model for evaluating industrial colour differences known as CIE94.⁵ This model captures the dependence of colour difference magnitude on the lightness, chroma, and hue of the sample. The CIE94 equation is recommended for a set of reference conditions, which differ significantly from our viewing geometry. We know that chromatic differences are more important in large regions than in small features and high frequency regions, where lightness differences are more important. Because the data we measured bears a qualitative similarity to CIE94, in that threshold colour differences increase with increasing C^* , we fit the data to a generalized CIE94 equation. We found a significant difference between the new equation and that derived for the CIE94 reference conditions.

Zhang and Wandell⁶ have proposed a spatial extension to CIELAB. Termed s-CIELAB, it brings results from chromatic (red/green and blue/yellow) spatial acuity experiments together with a well-known colour difference equation (ΔE^*_{ab}). Image colours are converted to an opponent colour space and the three opponent-colour channels are separately filtered. Two images filtered in this way are transformed to CIELAB and subtracted pixelwise from each other giving a map of Euclidean distance. A simple generalization of s-CIELAB, which we term s-CIELAB-94, improves the behaviour of s-CIELAB in the low frequency limit. Specifically, in the last stage of s-CIELAB, instead of using ΔE^*_{ab} to find the difference between two images, we use the CIE94 difference metric.

Experimental Method

Stimulus

For these experiments, we operated a SUN model GDM-20E20 monitor at 9500 K using the factory settings for brightness and contrast. We calibrated the monitor using a Minolta Model CA 100 CRT Color Analyzer. To determine the transformation from input digital value to output tristimulus value, we applied the gamma-gain-offset model described by Berns *et al.*⁷ For the $L^*a^*b^*$ stimuli in the preliminary data set, the maximum error between the desired and measured stimuli was $\Delta E_{ab} = 3.8$ and the rms error was $\Delta E_{ab} = 1.8$. This is the error in base colour. We expect the error in differences between line and base colours to be smaller.

Sixteen colour-normal (Ishihara test⁸) observers viewed stimuli illustrated in Figure 1 from a distance of 175cm. At 19.0 cm high, the entire stimulus subtended an angle of 6.2° , while the 0.09cm line subtended an angle of $1.8'$.

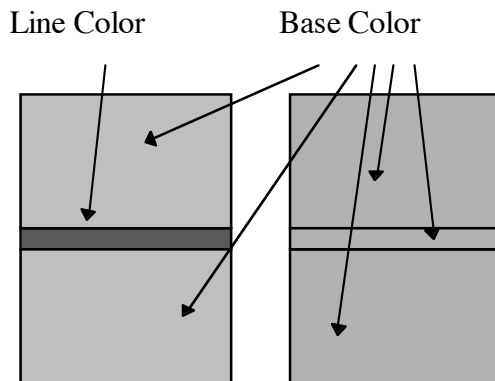


Figure 1. The geometry of the stimulus (not to scale).

The line in the stimulus appeared in either the left or the right hand rectangle, and its colour differed from that of large rectangle (the base colour) only in one of L^* , C^* or h_{ab} . The outlines on the rectangles are shown for illustrative purposes only.

We chose base colours to sample colour space well enough to identify any threshold dependencies on L^* , C^* or h_{ab} . The base colours appear in Table 1.

In a pilot study, we presented observers with line colours that differed from the base colour in both directions (e.g. greater and lesser C^*). Data indicated no difference between the two directions; hence we used only one direction (away from the neutral axis or away from the gamut boundary, if either of these might interfere.)

Sequencing

The initial design was a randomized double staircase forced-choice experiment⁹. To save observer time, we first used the method of adjustment to obtain two estimates of the threshold, and used them as starting points for the two

Table 1. Base colours used for the large patches in Figure 1.

Vary L^*			Vary h_{ab}			Vary C^*		
L^*	a^*	b^*	L^*	a^*	b^*	L^*	A^*	b^*
12.8	5.2	2.1	70	-5	0	70	-5	0
96.2	-2.1	5.2	88.6	-14.2	-5.9	92.4	-9.9	4.1
16.6	9.9	-4.1	20.4	5.9	-14.2	88.6	-14.2	-5.9
92.4	-9.9	4.1	84.8	-7.4	-18.0	84.8	-7.4	-18.0
88.6	-14.1	-5.9	81.0	8.8	-21.3	81.0	8.8	-21.3
20.4	5.9	-14.2	77.3	24.3	10.1	77.3	24.3	-10.1
84.8	-7.4	-18.0	73.5	26.7	11.1	31.8	-24.3	10.1
81.0	8.8	-21.3	69.7	11.9	28.7	73.5	26.7	11.1
77.3	24.3	-10.1	65.9	-12.6	31.3	35.5	-11.1	26.7
31.8	-24.3	10.1	62.1	-31.4	13.0	69.7	11.9	28.7
73.5	26.7	11.1	65.0	0.0	-45.0	43.1	30.3	12.6
35.5	-11.1	26.7	45.0	55.0	0.0	65.9	-12.6	30.3
39.3	11.9	28.7	84.0	0.0	70.0	46.9	31.4	-13.0
43.1	30.3	12.6	84.0	0.0	87.0	62.1	-31.4	13.0
65.9	-12.6	30.3	45.0	63.0	-82.0	50.7	13.3	-32.1
46.9	31.4	-13.0				54.5	-13.4	-32.3
62.1	-31.4	13.0				65.0	0.0	-45.0
50.7	13.3	-32.1				45.0	55.0	0.0
						84.0	0.0	70.0
						84.0	0.0	87.0
						45.0	63.0	-82.0

staircases. No data taken prior to the staircases was used in the analysis. Thus observers did not need to be particularly careful during the method-of-adjustment phase.

During the staircase (forced choice) phase, observers indicated on which side the line appeared, choosing arbitrarily when they could not see a line. We randomized the side on which the line was displayed and which of the two staircases was used in a given trial. The modified random number generator was biased in favor of choosing the staircase/side less frequently chosen in prior selections.

A staircase was considered above threshold if and only if 3 of the last 4, 5 of the last 7, or 6 of the last 9 responses were correct. Each of the two staircases reversed direction whenever it crossed threshold. On each reversal, the step size dropped by a factor of 0.625. The step size began at 0.015 of the possible range of values; the staircase ended when the step size reached 0.005 of the possible range. The largest range was less than 200; thus thresholds were measured to within a ΔE^*_{ab} of 1 or less. Intra- and inter-observer noise significantly exceeded this limit.

Analysis

Determining the Threshold

We determined the threshold based on 75% likelihood of a correct response. First, we sorted all responses for a given observer, base colour and direction of variation by ΔE^*_{ab} . (Since only one of L^* , C^* and h_{ab} varied, this resulted

in sorting by the amount of variation in that parameter). Then we replaced every response with the fraction correct in the five responses centred on it. We took the first 0.6 in the series when considered in order of decreasing ΔE_{ab}^* as just below threshold, while we took the 0.8 immediately preceding it as at threshold. After removing extreme outliers, we used the range mean of the central 75% of resulting thresholds to give the estimated threshold for each condition.

Qualitative Results

Initial results showed a substantial difference between thresholds for ΔL and ΔC or ΔH , with substantially less difference between ΔC and ΔH . Plotting the data, we found a qualitative agreement with CIE94, (i.e. only ΔC and ΔH depended on C^*). To test the hypothesis that CIE94 provides a good estimate of the visibility of a thin line, we plotted ΔC , ΔH , and ΔL against L^* , C^* and h_{ab} of the base colour. No dependence of ΔL on location in colour space is predicted, and no dependence of ΔC or ΔH on L^* or h_{ab} is predicted by CIE94. Thus any dependence on C^* must be significantly larger than any apparent dependence on L^* , in order to be meaningful.

As expected, there was no significant dependence on L^* , while there was a significant dependence on C^* . We also found a significant dependence on h_{ab} , not predicted by CIE94.

CIE94 Parameters

We expanded the CIE94 equation

$$\Delta E_{94} = ((\Delta L/S_L)^2 + (\Delta C/S_C)^2 + (\Delta H/S_H)^2)^{1/2}$$

to

$$\Delta E_{94} = ((\Delta L/(k_L(1+\alpha_L)))^2 + (\Delta C/(k_C(1+\alpha_C)))^2 + (\Delta H/(k_H(1+\alpha_H)))^2)^{1/2}$$

giving six free parameters. The CIE recommends that α_L is 0, and k_L is 1. We varied k_L so that the threshold of visibility was 1, but retained $\alpha_L = 0$. Also in the original formula, α_C and α_H are fixed at 0.015 and 0.045, respectively. We treated them as free parameters, in order to account for the non-reference geometry.

When ΔL and ΔH are 0, the difference equation is

$$\Delta E_{94} = \Delta C/(k_C(1+\alpha_C C^*)),$$

with a similar equation involving ΔH when the other two are 0. We used the chroma of the base colour for C^* in this equation. For threshold, we define $\Delta E_{94} = 1$. Re-arranging,

$$\Delta C = k_C + k_C \alpha_C C^*.$$

By regression analysis, we obtained the line of best fit for ΔC as a function of C^* ; from the slope and intercept we obtained values of k_C and $k_C \alpha_C$, and hence α_C . By the same method, we obtained values of k_H and α_H .

To study the relationship of ΔC and ΔH against h_{ab} we added an additional (periodic) function of h_{ab} to S_C and S_H ,

and manually optimized the parameters to minimize the rms error between the measured data and the thresholds predicted by the modified CIE94 equation. As modified, the equations became:

$$S_C = (1 + \alpha_C C^*)(1 + \beta_C((A_{1C} \cos(H^* - \phi_{1C})) + (A_{2C} \cos(2H^* - \phi_{2C}))))$$

$$S_H = (1 + \alpha_H C^*)(1 + \beta_H((A_{1H} \cos(H^* - \phi_{1H})) + (A_{2H} \cos(2H^* - \phi_{2H}))))$$

s-CIELAB Analysis

We obtained Matlab code for the s-CIELAB model from Xuemei Zhang's web page at Stanford University*.

In order to determine whether s-CIELAB accurately predicts the threshold results obtained in the experiment, we took the base stimulus (i.e. the image with no line present) as one image and the base plus threshold line stimulus as the second image. The 75% range mean was used for the line stimulus. We used these two images as input to the s-CIELAB code, with one modification: the final comparison was performed using the CIE94 colour difference equation (s-CIELAB-94). We used the pixel having the maximum error in the difference image as a metric for visual difference. We used the maximum error instead of the average error, since the images were identical over most of their area.

All the base/line colour image pairs have the same visual difference (equal to visual threshold in this case) so we would like to find a colour difference metric that gives the same value for all the thresholds collected. Since we found observers to be more sensitive to small changes in lightness than to changes in chroma or hue, we were interested to see whether s-CIELAB's different filtering of the achromatic and chromatic channels accounts for this.

We also determined the line colour necessary to give an s-CIELAB-94 difference of 1.0 for each of the base colours in the experiment, using binary search along the appropriate direction. We compared the predicted colours to the actual observer threshold line colours.

Results

ΔL

Plotting ΔL against L^* , C^* and h_{ab} showed no dependence. All three lines of best fit for ΔL against L^* , C^* and h_{ab} had slopes less than 0.015 and R^2 less than 0.23. The median ΔL value for the threshold was 1.36, with a standard deviation of 0.41. The lack of dependence of ΔL on location in colour space agrees with prior colour difference equations. Our experience with ΔL for large patches indicates a value less than 1 for a just noticeable difference; the elevated threshold for a thin line is consistent with s-CIELAB's prediction (blurring reduces the contrast).

* <http://white.stanford.edu/html/xmei/scielab/scielab.html>

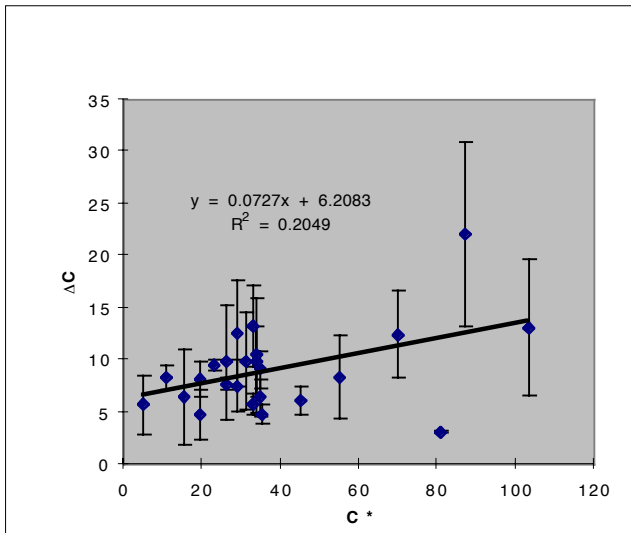


Figure 2. The threshold value of ΔC increases with increasing C^* . h_{ab} dependence largely explains apparent outliers. Error bars are 1 standard deviation of all data; points represent means of the central 75%.

ΔC

Plotting ΔC against L^* again showed no dependence. A line of best fit had slope less than 0.003 and $R^2 = 0.0002$. Plotting ΔC against C^* did show a dependence (Figure 2.) When we solved for the CIE94 parameters, we obtained values of $k_C = 6.21$ and $\alpha_C = 0.012$. The first of these is approximately 6 times the value given in CIE94, which we attribute to the geometry of the presentation. α_C is

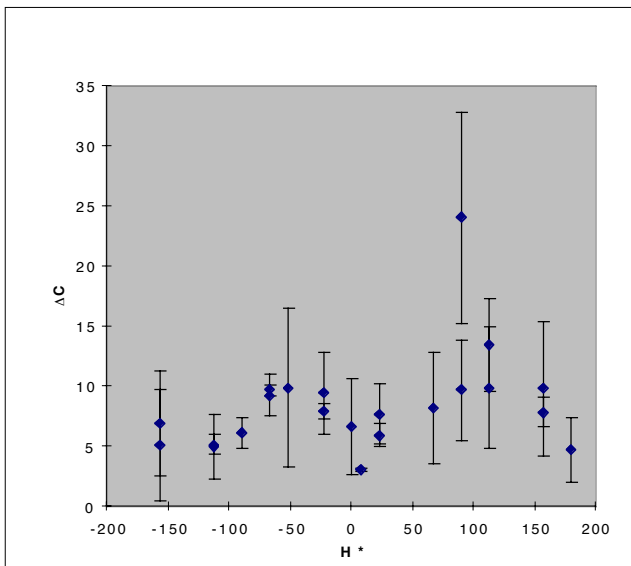


Figure 3. ΔC dependence on h_{ab} peaks at -50 and 110°

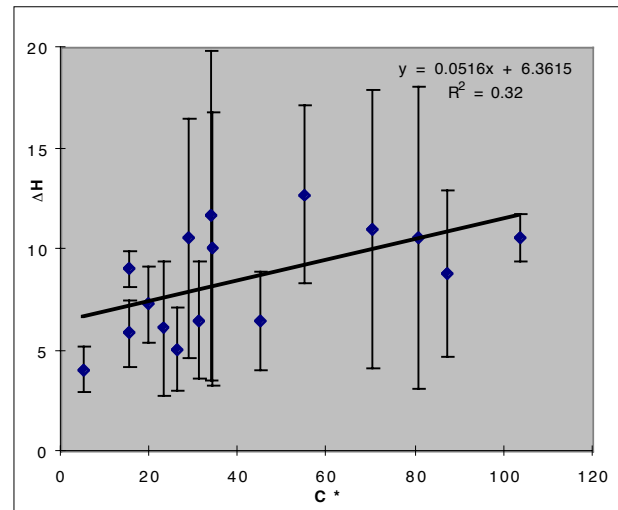


Figure 4. ΔH^* as a function of C^* follows a similar pattern to ΔC^*

approximately double the recommended value. The correlation coefficient for CIE94 against measured thresholds was 0.45, while the rms error between the CIE94 estimate of threshold and the mean measured threshold was 7.17. When the values of k_C and α_C are substituted into the CIE94 equation, the correlation coefficient remains the same (as it should, since the character of the function hasn't changed), but the rms error drops to 4.4.

Figure 3 shows the dependence of ΔC on hue. There appears to be a periodic variation with two peaks, and a peak-to-peak variation of roughly 5, enough to be significant. With the modified equation:

$$S_C = (1 + 0.012C^*)(1 + 0.08((3.6 \cos(H^* - 91^\circ)) + (4.1 \cos(2H^* - 228^\circ))))$$

the correlation coefficient improved to 0.825, while the rms error dropped to 3.34. Much of the apparent scatter in the

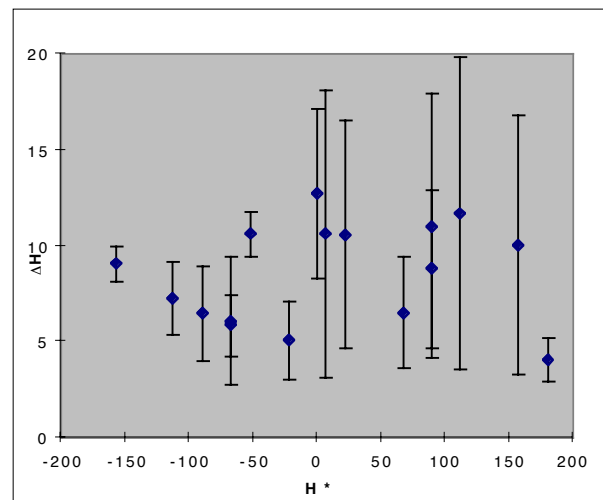


Figure 5. ΔH^* against h_{ab} follows the same pattern as ΔC .

data means comes from the fact that multiple values of h_{ab} appear for any given value of C^* in the graphs with C^* on the abscissa, and vice versa.

ΔH^*

Plotting ΔH^* against L^* showed no dependence (slope < 0.007 , $R^2 < 0.002$); ΔH^* against h_{ab} was qualitatively similar to ΔC against h_{ab} (Figure. 4.) Plotting ΔH^* against C^* did show a dependence, particularly for large C^* (Figure. 5) Solving for CIE94 parameters gave values of $k_H = 6.36$ and $\alpha_H = 0.008$, only slightly different from the parameters for ΔC . The rms error improved from 6.81 to 3.04 by changing the parameters k_H and α_H .

Again, applying the more detailed optimization improves both the correlation coefficient and the rms error, but less dramatically. With the modified

$$S_H = (1 + 0.0081C^*)(1 + 0.004((9.1 \cos(H^* - 69^\circ)) + (3.2 \cos(2H^* - 316^\circ))))$$

the correlation coefficient rises to 0.65 from 0.57, while the rms error drops to 2.98. In this case, the improvement due to the h_{ab} term is less dramatic.

s-CIELAB Predictions

One measure of performance for a metric is the variance in predicted colour differences for the colours measured to be at threshold. A perfect color difference equation would be expected to give the same value for all base/line colour pairs since they all had the same visual difference. We found that s-CIELAB-94 gives a much more uniform error predictor than CIELAB or s-CIELAB, and is approximately equivalent to the optimized CIE94 type equation described previously. Table 2 shows the mean and standard deviation of the various metrics. This table shows s-CIELAB-94 performs nearly as well as the model that was optimized for the given data set.

Table 2. Mean and standard deviations of various colour difference formulae over the range means of all base/line pairs.

Metric	Mean	Std. Deviation
ΔE^*_{ab}	6.625	4.861
ΔE_{94}	3.455	2.204
Modified ΔE_{94}	1.027	0.310
s-CIELAB-94	0.967	0.403

To measure the performance of s-CIELAB as a predictor of observed thresholds, we calculated the line colour that would equal a just-noticeable difference (jnd) from the base colour using s-CIELAB-94. For the results shown in Figure 6, the average jnd corresponded to an s-CIELAB-94 value of 0.967, which we took to be within noise of 1.0. As shown in Figure. 6, s-CIELAB-94 as a threshold predictor performs quite well. The slope would be closer to 1 had we used the value of 0.967, but the correlation coefficient would be unchanged. For comparison

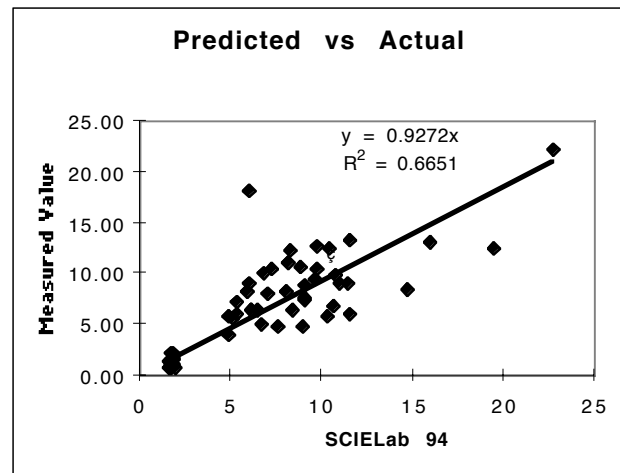


Figure 6. Range mean thresholds vs s-CIELAB predictions. A perfect fit would have unit slope and R^2 values. The threshold for s-CIELAB was chosen arbitrarily at 1.0; a different slope would bring the slope closer to unity.

Figure 7, shows the fully optimized CIE94 model performance. By design, the slope is very close to unity. The correlation coefficient is significantly higher than that for s-CIELAB-94. Thus the full model fits the data better than does s-CIELAB-94, which already fits the data quite well. s-CIELAB-94 has the advantage of applying to arbitrary geometries, while the full model only applies to the geometry used in this experiment.

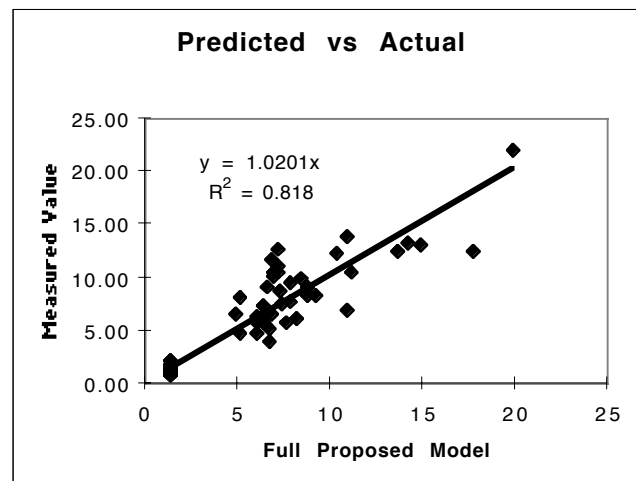


Figure 7. When the measured values are plotted against the proposed model, the fit improves significantly; this is to be expected since the model was designed to fit this data set.

Conclusion

The CIE94 formula provides a good starting point for modeling the visibility of thin lines against a solid background. The specific parameters appear to be functions of spatial frequency. For the specific geometry we used, characteristic of thin linear defects in print material, the parameters we found fit best give the equation

$$(\Delta E_{94} = ((\Delta L/1.36)^2 + (\Delta C/6.23S_C)^2 + (\Delta H/6.36S_H)^2)^{1/2}$$

with

$$S_C = (1 + 0.0117 C^*)(1 + 0.08 ((3.6 \cos(H^* - 91^\circ)) + (4.1 \cos(2H^* - 228^\circ))))$$

and

$$S_H = (1 + 0.0081 C^*)(1 + 0.004 ((9.1 \cos(H^* - 69^\circ)) + (3.2 \cos(2H^* - 316^\circ))))$$

We suspect that the CIE94 parameters are all functions of spatial frequency. It is well known that the threshold of lightness visibility for neutral greys is a function of spatial frequency, so this is to be expected.

s-CIELAB used with the CIE94 color difference metric offers an accurate way to model the visibility of thin lines on a solid background. Further testing will be needed to assure that this technique works for lines of different thickness or patterns of different geometries. However, the fact that the metric could accurately predict the results of this study without optimization indicates promise.

While we only explored a single geometry (hence a single spatial frequency distribution), we took base colours from a broad cross section of colour space, rather than only the neutral axis or a* or b* axis. We hope to see more work mapping the spatial frequency response of the visual system to locations throughout colour space.

References

- ¹ Robson, J.C. "Spatial and temporal contrast-sensitivity functions of the visual system", *Journal of the Optical Society of America* **56**, 1141-1142, (1966).
- ² Kelly, D.H., "Spatiotemporal variation of chromatic and achromatic contrast thresholds" *Journal of the Optical Society of America* **73**, 742-750, (1983).
- ³ Noorlander, C., M.J.G. Heuts and J.J. Koenderink, "Sensitivity to spatiotemporal combined luminance and chromatic contrast", *Journal of the Optical Society of America*, **71**pp. 453-459, 1981
- ⁴ Mullen, K.T., "The contrast sensitivity of human colour vision to red-green and blue-yellow chromatic gratings", *J. Physiology*, **359**pp. 381-400, 1985
- ⁵ Commission Internationale de l'Eclairage (CIE), *Technical Report: Industrial Colour-Difference Evaluation, Publication CIE 116-1995*, Bureau Central de la CIE, (1995).
- ⁶ Zhang, X. and B. Wandell, "A spatial extension of CIELAB for digital color image reproduction" *SID Symposium Technical Digest* **27**, 731-734 (1996).
- ⁷ Berns, R.S., Motta, R.J. and Gorzynski, M.E., CRT Colorimetry. Part 1: Theory and Practice, *Color Res. Appl.* **18**, 299-314 (1993).
- ⁸ Ishihara, S. *Tests for Colour-Blindness*, Kanehara Shuppen, Tokyo, 1977
- ⁹ Cornsweet, T.N. "The staircase method in psychophysics", *American Journal of Psychology* **75**, 485-491 (1962).